

Supporting Information

Phosphorous oxide clusters stabilized by carbon nanotubes for selective isomerization and dehydrogenation of β -isopentene

Rui Huang,^[a,b] Jia Wang,^[a] Bingsen Zhang,^[a] Kuang-Hsu Wu,^[a,d] Yajie Zhang,^[a] and Dang Sheng Su^{*[a,c]}

[a] Dr. R. Huang, Dr. J. Wang, Prof. B. S. Zhang, Dr. K. H. Wu, Y. J. Zhang, Prof. D. S. Su
Shenyang National Laboratory for Materials Science
Institute of Metal Research, Chinese Academy of Sciences
Wenhua Road 72, Shenyang, 110016 (PR. China)
E-mail: rhuanges17@hotmail.com; dangsheng@fhi-berlin.mpg.de

[b] Dr. R. Huang, Dr. J. Wang
State Key Laboratory for Oxo Synthesis and Selective Oxidation, Suzhou Research Institute of
LICP, Lanzhou Institute of Chemical Physics (LICP), Chinese Academy of Sciences, Lanzhou
730000, China.

[c] Prof. D. S. Su
Energy Research Resources Division, Dalian Institute of Chemical Physics, Chinese Academy of
Sciences
Zhongshan Road 457, Dalian 116023 (PR. China)

[d] Dr. K.H. Wu
School of Chemical Engineering
The University of New South Wales
Kensington, Sydney, NSW 2052 (Australia)

Experimental Section

Preparation of catalysts. The heat-treated carbon nanotubes (A1500) annealed at 1500 °C in argon (Ar) for 5 h, which were used as an inert carbon carrier for supporting the active ingredients. The supported VO_x-A1500 and PO_x-A1500 catalysts were prepared by incipient wetness impregnation combined with ultrasonic dispersion. The aqueous solutions of NH₄VO₃ (>99%, Aldrich, Inc.) or (NH₄)₂HPO₄ (>99%, Aldrich, Inc.) was added oxalic acid (>99%, Aldrich, Inc.) in a 1:3 molar ratio in order to ensure dissolution of ammonium salt precursors. The supports were soaked in the above aqueous solution and stirred ultrasonically until all the water to be evaporated. The impregnated samples were dried in air at 80 °C for 12 h and crushed, followed by heat-treated at 500 °C in Ar for 3 h. The TPP-A1500 catalyst was prepared by chemical vapor deposition using triphenylphosphine (TPP, >99%, Aldrich, Inc.) as phosphorous source in two continuous furnaces, shown in Figure S1. TPP was vaporized (Furnace I, 380 °C for 2 h) and carried to the preheated supports (Furnace II, 500 °C for 3 h) by an Ar flow of 50 ml/min.

Characterization. Surface chemistry properties of the samples were conducted by using an ESCALAB 250 instrument with Al K α radiation (1486.6 eV, 15 kV, 10 mA, 150 W). X-ray diffraction (XRD) patterns were recorded by a D/max 2400 diffractometer (JEOL Ltd., Japan) with Cu K α (40 kV, 40 mA) radiation. The acidity of catalysts was measured by ammonia temperature-programmed desorption (NH₃-TPD). 0.05 g of sample was used in each test and was placed in a vertically positioned quartz tubular reactor. It was firstly adsorbed to balance under 5% NH₃/He at 25°C and then desorbed from 25 to 900 °C with a ramp rate of 5°C/min. The released NH₃ ($m/z=17$) was monitored by an in-situ quadrupole mass spectrometer (MS, Pfeiffer-Balzer Omnistar). Transmission electron microscopy (TEM) and high-angle annular dark field scanning TEM (HAADF-STEM) images were acquired by using an FEI Tecnai G2 F20 microscope equipped with HAADF-STEM detector and operated at 200 kV.

Catalytic reactions. Each catalyst (0.1 g, 100×400 μ m) mixed with quartz sand (1 g) was placed in a quartz tubular reactor for the reaction test. It was then kept at 400°C in a 20 ml/min flow with fixed ratio of 2M2B/O₂/He (1:1:18) until constant conversion was achieved. The different conversions were obtained by variation of reaction temperature at the range of 400-450 °C. The reactants and products were analysed by using an on-line gas chromatography system (Agilent 7890A) with two Hayesep Q columns, a HP-PLOT/Al₂O₃ column (50 m 0.32 mm 8 mm) and a molecular sieve column. CO and CO₂ were detected with TCD detector, and hydrocarbons were detected with FID detector.

Calculation methods. The conversion (X_{2M2B}), product selectivity (S_p), yield (Y_p) and reaction rate (R_i) is calculated by formula (1), (2), (3) and (4), respectively. Among them, “ F , C , w ” denotes flow rate (mL min⁻¹), concentration (v.v %) and catalyst weight (g), respectively. “ i ” means any product from the reaction system and “ p ” only represents one specific product, whereas “ j ” denotes any specific

component including reactant or product. For consumption rate of reactant, the formula (4) is calculated by " X_{2M2B} ", whereas the formation rate of product is obtained by " Y_p ". " Σ " means summation.

$$\text{Conversion: } X_{2M2B} = \frac{F_{2M2B} \times (C_{2M2B, \text{inlet}} - C_{2M2B, \text{outlet}})}{F_{2M2B} \times C_{2M2B, \text{inlet}}} \times 100\% \quad (1)$$

$$\text{Selectivity: } S_p = \frac{C_{p, \text{outlet}}}{\Sigma C_{i, \text{outlet}}} \times 100\% \quad (2)$$

$$\text{Yield: } Y_p = X_{2M2B} \times S_p \times 100\% \quad (3)$$

$$\text{Reaction rate: } R_j = \frac{F_{2M2B} \times C_{2M2B, \text{inlet}} \times X_{2M2B} \text{ (or } Y_p)}{22.4 \times w_{cat.} \times t} \quad (4)$$

Table S1. Blank test for the homogeneous conversion of 2M2B at different reaction temperature.

Temperature (°C)	X_{2M2B} (%)	Y_{iso} (%)	Y_{deh} (%)	Y_{com} (%)
350	0.14	0	0.14	0
450	0.71	0	0.71	0

Table S2. Typical XPS fitting data of different samples from Figure 3.

Sample	A1500		TPP-A1500		POx-A1500		K-POx-A1500		P ₂ O ₅	
Component	BE ^a (eV)	PA ^b (%)	BE (eV)	PA (%)	BE (eV)	PA (%)	BE (eV)	PA (%)	BE (eV)	PA (%)
C _C (at %) ^c	98.03		89.25		83.07		95.04		50.07	
C _O (at %)	1.97		9.63		15.37		4.45		39.94	
C _P (at %)	0.00		1.12		1.56		0.51		9.99	
=O ^d	531.4	4.36	531.4	21.99	531.4	27.84	531.4	2.64	531.2	14.24
-O-	533.1	95.64	533.3	78.01	533.2	69.34	533.1	97.35	532.7	85.76
H ₂ O/O ₂	535.7	0.00	535.7	0.00	536.1	2.82	535.7	0.00	535.7	0.00
C-P ^e			132.5	38.75						
PP			133.5	61.25	133.7	56.59	133.7	85.75	133.7	32.13
MP					134.6	43.41	134.6	14.25	134.5	51.91
P ₂ O ₅									135.4	15.96

^a binding energy; ^b percentage of peak area of each component from XPS fitting results in Figure 3; ^c "C_C, C_O, C_P" represents the content of carbon, oxygen and phosphorus atom in each sample. ^d "=O, -O-, H₂O/O₂" denotes the three components (double bonded oxygen, single bonded oxygen and adsorbed H₂O/O₂) from the fitting O1s spectra (Figure 3b). ^e "C-P, PP, MP and P₂O₅" is the four components (C-P bond, polyphosphate, monophosphate and phosphorus pentoxide structure) from the fitting P2p spectra (Figure 3c).

Table S3. XPS fitting data of different TPP- and POx-A1500 samples from Figure 3 and Figure 4.

	A1500	1POx ^a	3POx	5POx	10POx	TPP	K-POx
$C_C(\text{at}\%)^b$	98.03	97.63	94.47	91.37	83.07 (80.19) ^c	89.25	95.04
$C_P(\text{at}\%)$	0.00	0.12	0.31	0.59	1.56 (1.29)	1.12	0.51
$C_{PP}(\text{at}\%)$	0.00	0.04	0.19	0.44	0.88	0.69	0.44
$C_{MP}(\text{at}\%)$	0.00	0.08	0.12	0.15	0.68	0.00	0.07
$\%_{PP}^d$	0.00	0.30	0.62	0.75	0.57	0.61	0.86
$\%_{MP}$	0.00	0.70	0.38	0.25	0.43	0.00	0.14
$C_O(\text{at}\%)$	1.97	2.25	5.22	8.04	15.37 (18.52)	9.63	4.45
$C_{=O}(\text{at}\%)$	0.09	0.18	0.86	1.85	4.28	2.12	0.12
$C_{-O}(\text{at}\%)$	1.88	1.17	4.01	5.49	10.66	7.51	4.33
$\%_{=O}$	0.04	0.08	0.17	0.23	0.28	0.22	0.03
$\%_{-O-}$	0.96	0.52	0.77	0.68	0.69	0.78	0.97
$R_{\text{total}}(\text{mmol g}^{-1} \text{h}^{-1})^e$	2.43	4.25	4.70	4.85	5.26	4.16	1.81
$R_{\text{ISO}}(\text{mmol g}^{-1} \text{h}^{-1})$	2.05	3.88	3.94	3.86	3.98	3.28	0.54
$R_{\text{DEH}}(\text{mmol g}^{-1} \text{h}^{-1})$	0.31	0.33	0.67	0.79	1.04	0.64	0.07
$R_{\text{COM}}(\text{mmol g}^{-1} \text{h}^{-1})$	0.07	0.04	0.09	0.19	0.24	0.24	1.19
$S_{\text{ISO}}(\%)^f$	84.35	91.27	83.87	79.71	75.63	78.82	30.15
$S_{\text{DEH}}(\%)$	12.89	7.84	14.20	16.30	19.85	15.37	3.87
$S_{\text{COM}}(\%)$	2.76	0.89	1.93	3.99	4.52	5.81	65.98

^a "1POx" represents the 1POx-A1500 sample with 1% phosphorus content in theory; ^b " C_C , C_P , C_{PP} , C_{MP} , C_O , $C_{=O}$, C_{-O-} " corresponds to the content of carbon atom, phosphorus atom, polyphosphate structure, monophosphate structure, oxygen atom, double bonded oxygen linkage and oxygen single bond in each sample from XPS fitting data in Figure 3 and Figure 4; ^c the value of spent sample; ^d " $\%_{PP}$, $\%_{MP}$ " denotes the proportion of polyphosphate structure and monophosphate structure to all P atoms in each sample, and also " $\%_{=O}$, $\%_{-O-}$ " means the proportion of double bonded oxygen and single bonded oxygen to all O atoms in each sample; ^e " R_{total} , R_{ISO} , R_{DEH} , R_{COM} " indicates the reaction rate of all products(total), isomerized products (iso, 2M1B and 3M1B), dehydrogenated products (deh, 2M-1, 3-Butadiene) and combusted products (com, CO and CO₂), and it was acquired from the data at 400 °C in Figure 2 and Figure S2; ^f " S_{ISO} , S_{DEH} , S_{COM} " is the selectivity for isomerization, dehydrogenation and combustion.

Table S4. The structure-activity relations based on the linear and non-linear analysis from Figure S5.

Entry	Linear regression of $y=kx+b$				Non-linear shift from exceptional samples		
	y	x	R ²	k	Downward shift		Upward Shift
1	R_{total}	C=O	0.90	0.22	A1500	TPP	K-POx
2		C-O-	0.96	0.10	A1500	TPP	K-POx
3		C _O	0.93	0.07	A1500	TPP	K-POx
4		C _{PP}	0.92	1.08	A1500	TPP	K-POx
5		C _P	0.86	0.60	A1500	TPP	K-POx
6		C _{MP}	0.71	1.24	A1500	TPP	K-POx
7	R_{ISO}	C _{MP}	0.56	0.14	A1500	TPP	K-POx
8		C _P	0.45	0.05	A1500	TPP	K-POx
9		C _{PP}	0.03	0.08	A1500	TPP	K-POx
10		C=O	0.40	0.02	A1500	TPP	K-POx
11		C-O-	0.46	0.01	A1500	TPP	K-POx
12		C _O	0.41	0.01	A1500	TPP	K-POx
13	R_{DEH}	C=O	0.86	0.16			K-POx
14		C-O-	0.83	0.07			K-POx
15		C _O	0.87	0.05			K-POx
16		C _{PP}	0.76	0.67			K-POx
17		C _P	0.72	0.39			K-POx
18		C _{MP}	0.63	0.86			K-POx
19	R_{COM}	C _{PP}	0.92	0.24			K-POx
20		C _P	0.84	0.14			K-POx
21		C _{MP}	0.22	0.17			K-POx
22		C-O-	0.86	0.02			K-POx
23		C=O	0.76	0.05			K-POx
24		C _O	0.82	0.02			K-POx
25	S_{ISO}	% _O	0.99	-79.40	A1500		K-POx
26		% _{O-}	0.47	-39.90			A1500
27		% _{MP}	0.44	15.59			K-POx
28		% _{PP}	0.30	-10.79			K-POx
29	S_{DEH}	% _O	0.98	60.85			A1500
30		% _{O-}	0.60	-18.61	1POx		K-POx
31		% _{PP}	0.30	7.85			K-POx
32		% _{MP}	0.28	-9.05			K-POx
33	S_{COM}	% _{MP}	0.71	-6.55			K-POx
34		% _O	0.51	14.10			K-POx
35		% _{PP}	0.20	2.95			K-POx
36		% _{O-}	0.08	3.67			K-POx

All the parameters originated from Figure S5. The explanatory variables (x) of each dependent variable (y) are sorted by the correlation coefficient (R^2) and the slope (k) of lines. The PO_x-A1500 samples without potassium addition nearly meet the linear relationship. "Downward shift"/"Upward shift" indicating the value of dependent variable is less /more than the value on the line regression, in which the corresponding structure variable of special sample is un/favorable for that catalytic function.

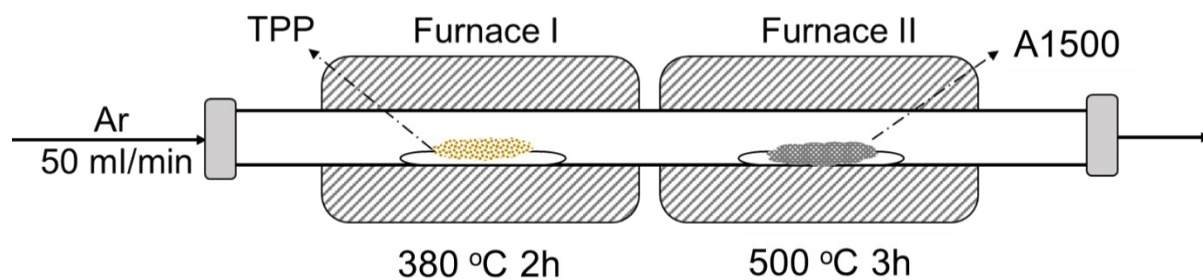


Figure S1 Schematic diagram for the preparation of TPP-A1500 via chemical vapour desorption.

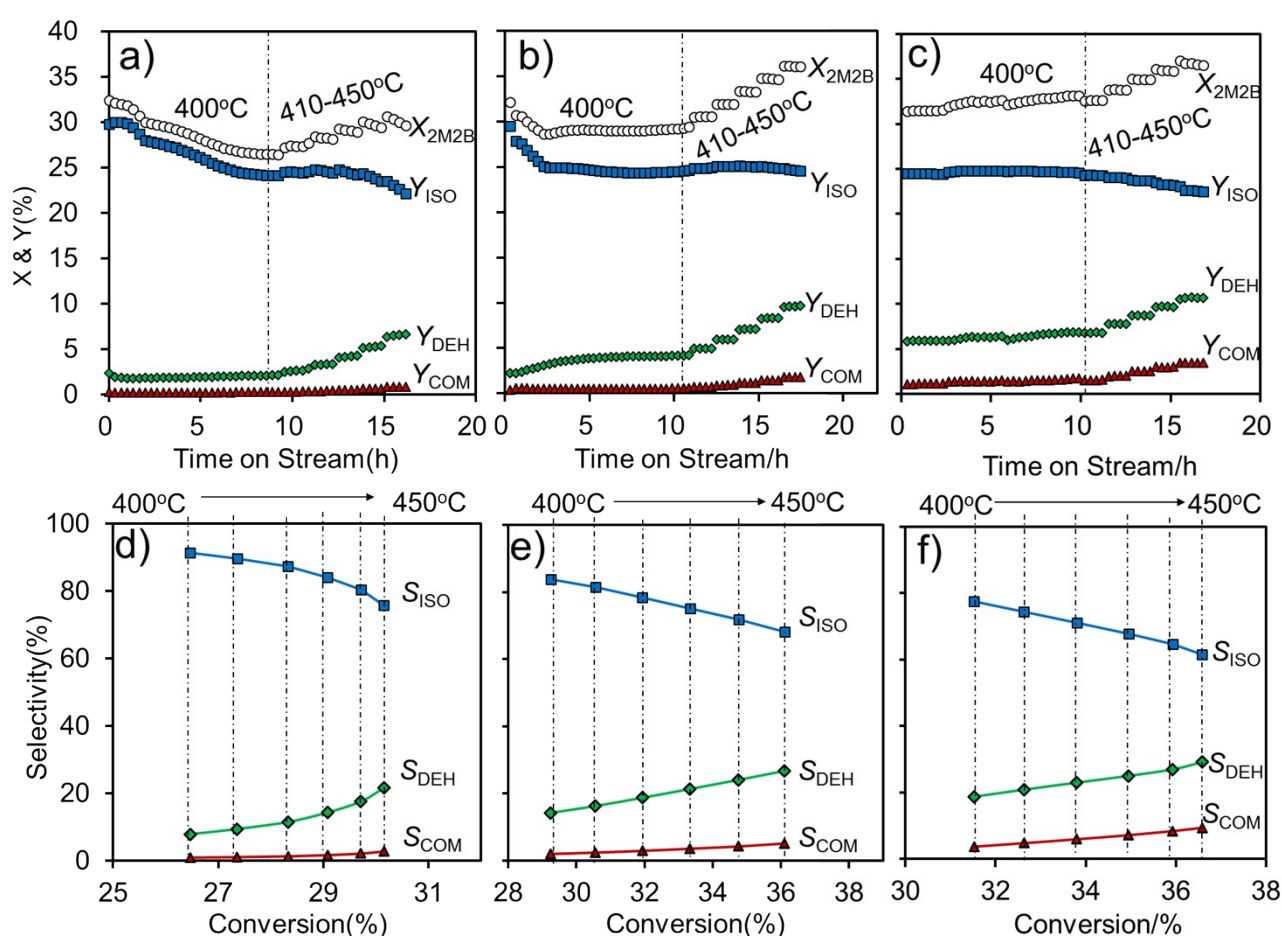


Figure S2 Catalytic performance for oxidative conversion of β -isopentene (2M2B) over different catalysts. (a-c) Conversion of 2M2B (\circ : X_{2M2B}) and yield of products as a function of time on stream over 1POx-A1500 (a), 3POx-A1500 (b) and 5POx-A1500 (c) at isoweight of catalyst (0.1 g, 12 L g⁻¹h⁻¹, 2M2B:O₂:He=1:1:18). \blacksquare : Y_{ISO} , the yield of isomerized products containing 2-methyl-1-butene (2M1B) and less 3-methyl-1-butene (3M1B); \blacklozenge : Y_{DEH} , the yield of dehydrogenated product containing 2-methyl-1, 3-butadiene (2M-1,3-Butadiene); \blacktriangle : Y_{COM} , the yield of combusted products containing CO and CO₂.

(d-f) The product selectivity as a function of 2M2B conversion over 1PO_x-A1500 (d), 3PO_x-A1500 (e) and 5PO_x-A1500 (f).

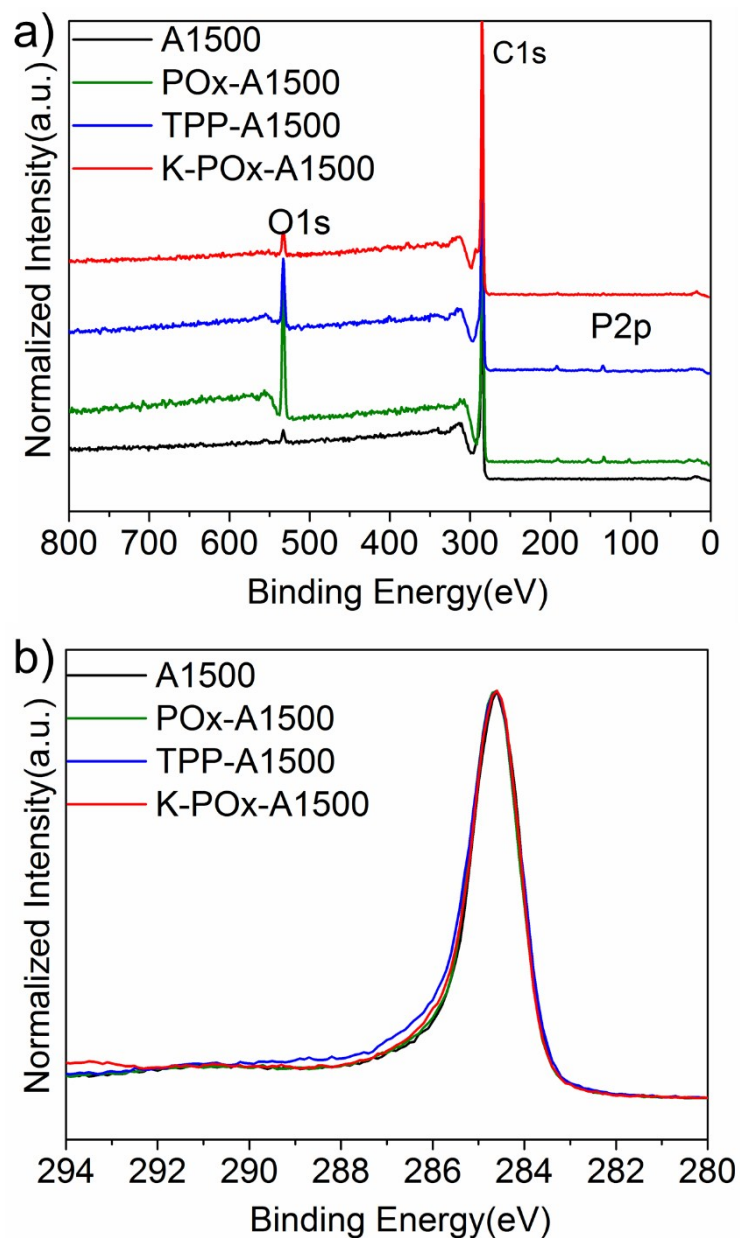


Figure S3 XPS survey spectra (a) and C1s spectra (b) of different samples. The survey spectra (Figure S3a) of PO_x-A1500 confirm the neat presence of carbon, oxygen and phosphorus elements. In the C 1s spectra (Figure S3b), no change in the binding energy (BE) could be identified before and after P-modification in the C 1s spectra.

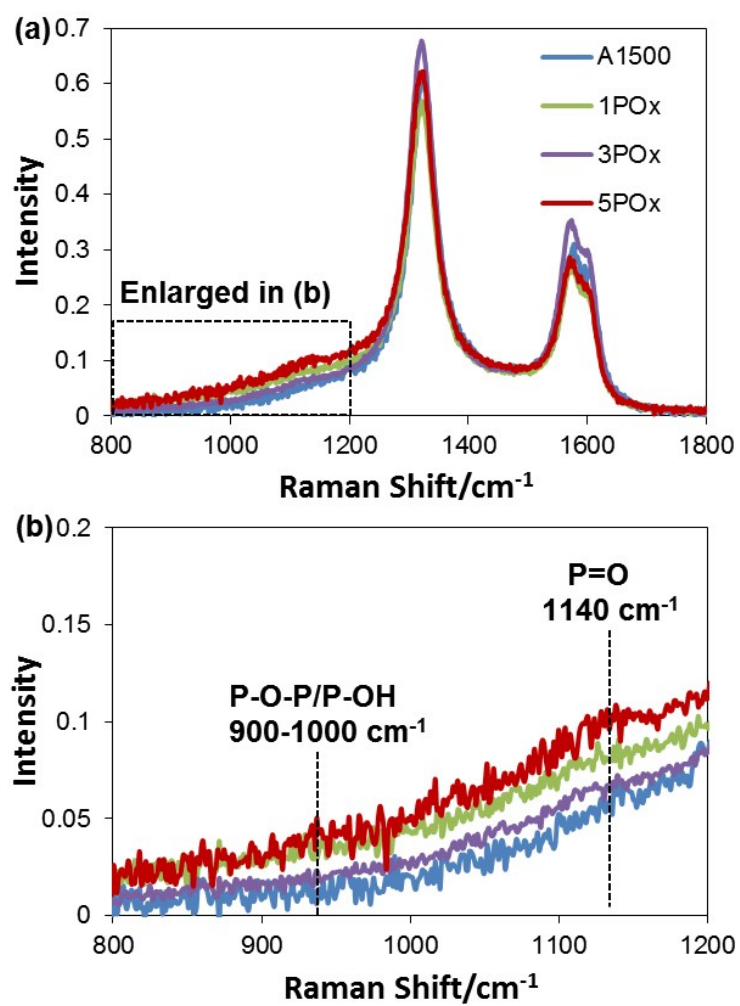


Figure S4 Overlay of Raman spectra for phosphate modified carbon nanotubes.

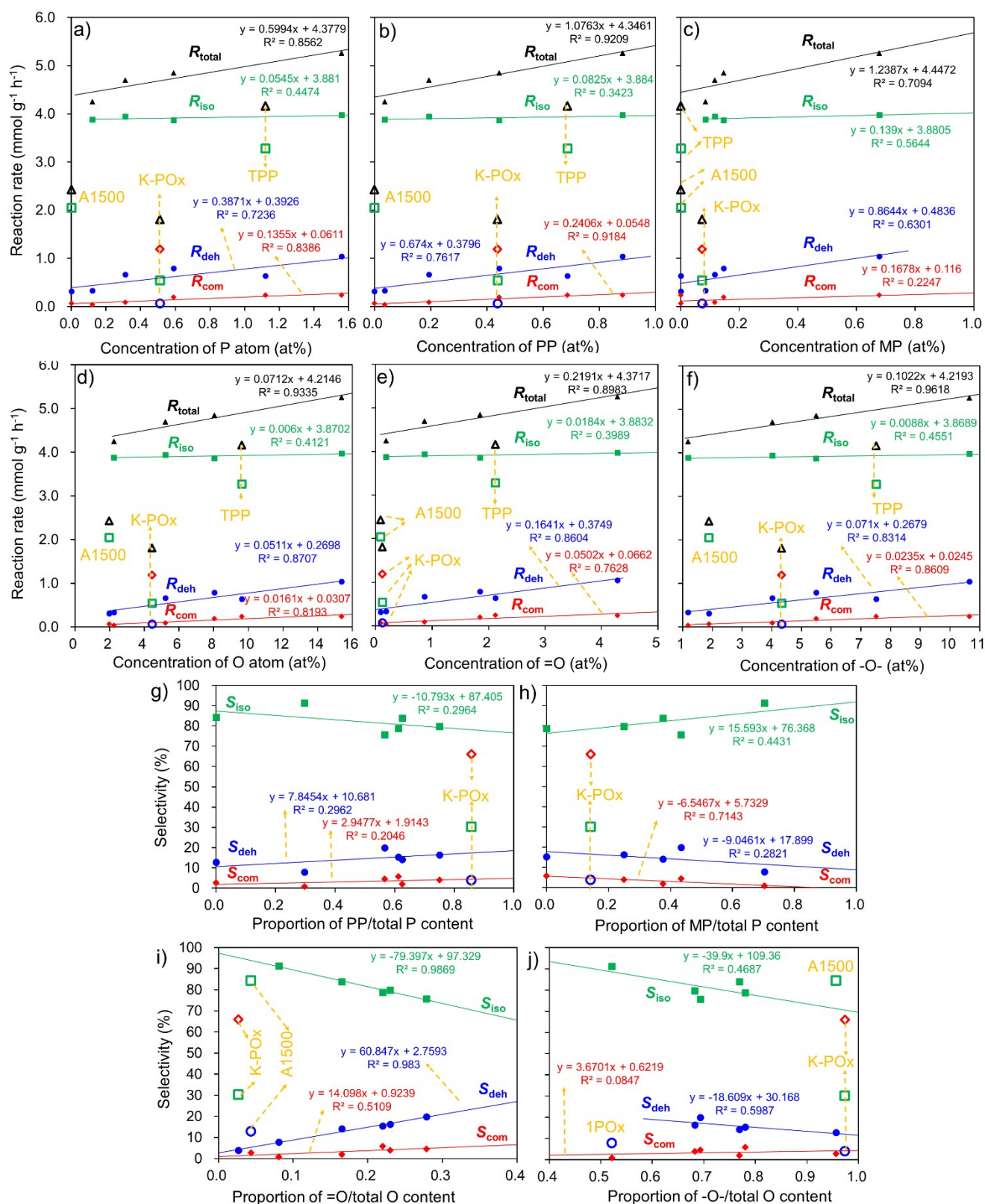


Figure S5 Linear and non-linear correlation between the catalytic function and the structure properties of samples.

Linear regression (Figure S5) was used to model the relationship between the catalytic function (dependent variable, y) and the structure variables (explanatory variable, x) by fitting a linear equation ($y=kx+b$) to the obtained data of 7 samples (A1500, TPP-A1500, 1POx-A1500, 3POx-A1500, 5POx-A1500, 10POx-A1500, K-10POx-A1500) in Table S3. The correlation coefficient (R^2) is a value between 0 and 1 indicating the strength of the association of the two variables. The slope of the line is k and b is the intercept. Most points meet the linear relationship between two variable pairs while a few outliers deviate from the line indicating the presence of exceptional samples (labelled in Figure). All these parameters and the direction of outliers deviating from the line have been summarized in Table S4. (a) y : total reaction rate (R_{total}), isomerization rate (R_{iso}), dehydrogenation rate (R_{deh}), combustion rate (R_{com}), x : the content of P atom in each sample (C_{P} , at %); (b) y : R_{total} , R_{iso} , R_{deh} , R_{com} , x : the content of polyphosphate structure in each sample (C_{PP}); (c) y : R_{total} , R_{iso} , R_{deh} , R_{com} , x : the content of monophosphate structure in each sample (C_{MP}); (d) y : R_{total} , R_{iso} , R_{deh} , R_{com} , x : the content of O atom in each sample (C_{O}); (e) y : R_{total} , R_{iso} , R_{deh} , R_{com} , x : the content of oxygen double bonds in each sample ($C_{=\text{O}}$); (f) y : R_{total} , R_{iso} , R_{deh} , R_{com} , x : the content of oxygen single bonds in each sample ($C_{-\text{O}-}$); (g) y : isomerized selectivity (S_{iso}), dehydrogenated selectivity (S_{deh}), combusted selectivity (S_{com}), x : the proportion of polyphosphate/total P atom (%PP); (h) y : S_{iso} , S_{deh} , S_{com} , x : the proportion of monophosphate/total P atom (%MP); (i) y : S_{iso} , S_{deh} , S_{com} , x : the proportion of oxygen double bonds/total O atom (% $_{=\text{O}}$); (j) y : S_{iso} , S_{deh} , S_{com} , x : the proportion of oxygen single bonds/total O atom (% $_{-\text{O}-}$).